PHYSICAL REVIEW C VOLUME 20, NUMBER 1 JULY 1979

Effect of number conservation on high spin states and nuclear deformation

M. R. Gunye
Bhabha Atomic Research Centre, Trombay, Bombay-85, India

C. S. Warke
Tata Institute of Fundamental Research, Colaba, Bombay-5, India

(Received 5 December 1978)

The high spin yrast states up to $J = 20^+$ in ^{158,160,162}Er are studied in the framework of microscopic variational approach by employing the Hamiltonian with quadrupole plus pairing interactions. The effect of number conservation on deformation, calculated energy spectra and $B(E2)$ values is investigated. It is observed that the results are quite sensitive to the number conservation. The results of the calculations are in better agreement with the corresponding experimental data as compared to those obtained without number conservation.

[NUCLEAR STRUCTURE Er Isotopes: calculated energy spectra, quadrupole moments and $B(E2)$. Variation after projection with number conservation in each state.]

I. INTRODUCTION

The transfer of large angular momentum and energy to the resulting final nucleus in the heavy ion reaction has made it possible to investigate high spin states in nuclei. A large amount of experimental data on the excitation energies and the $B(E2)$ values for the cascading γ transitions from these high spin states were accumulated during the last few years. The earlier macroscopic calculations[1] based on the Bohr-Mottelson collective model gave a qualitative explanation of the observed energy spacings. The observed deviation from the rotational character of the energy spectra was predicted earlier by Mottelson and Valatin[2] as a result of a phase transition caused by the vanishing of the pairing gap above a certain critical value of the angular momentum. The deviation from the rotational spectrum was also qualitatively explained in an alternative approach by Stephens and Simon[3] in terms of a band-crossing phenomenon in which the band intersecting the ground band becomes the yrast band for high spin states. It is of interest to gain an insight into the intrinsic nuclear structure of these high spin states. However, the drawback of the phenomenological approaches is that they require some relevant parameters to be fitted for each nucleus in order to explain the experimental data quantitatively. Some attempts[4] have been made recently to formulate the problem of high spin spectroscopy using the many-body variational methods with constraints. These approaches resort to simplifying approximations[4] regarding angular momentum conservation leading to errors which could be of the same order of magnitude as the observed energy differences to be explained. Moreover, within the framework of these constrained variational calculations,[4] one cannot calculate the $B(E2)$ values of the cascading γ transitions to test the validity of the theory by comparison with the corresponding experimental values.

In spite of the attempts made during the last few years, one has not yet succeeded in predicting the energy spectra of high spin states with the same accuracy as in the case of low-lying nuclear states using theoretical formalisms with a minimum number of parameters. The shell model, the collective model, and the projected Hartree-Fock formulation give a good account of the low-lying nuclear states. There have been, so far, very few attempts[5,6] to explain the spectroscopy of high spin states based on many-body variational formalism with good angular momentum. This is obviously due to the fact that such a collective phenomenon arising out of the coherent dynamical behavior of many nucleons is difficult to treat in a microscopic many-body theory. In a variational formalism, however, it is possible to devise reasonable approaches to cope with the complexity of many-body systems in a large configuration space. The success of such calculations in quantitatively explaining the observed energy spectra and $B(E2)$ values would enhance the confidence in variational projection formalism. The projected Hartree-Fock-Bogolubov (HFB) method is being used recently to understand the structure of high spin states in nuclei. Apart from the complications of angular momentum

projection in a large configuration space, there is yet another complication due to the number projection from the variational HFB state. The effect of number projection on the computed energy spectra has been estimated[7] by approximately evaluating the integral appearing in the number projection calculation. This approximate treatment,[7] however, does not eliminate the total mixing amplitude of all the numbers to a desired accuracy in the projected wave function. We had previously studied[6] the high spin states in a few rare-earth nuclei in the variational projection approach without number projection. The aim of this paper is to study the effect of number conservation on the calculated energy spectra and the $B(E2)$ values. It is of vital interest to know whether the number conservation improves the quality of agreement between the theoretical and experimental results.

The theoretical formulation with the mathematical expressions required in the calculation of energy, quadrupole moment, and $B(E2)$ values is given in Sec. II. The results obtained by applying this theory to the three nuclei ^{158,160,162}Er are discussed in Sec. III. The conclusions are presented in Sec. IV.

II. THEORETICAL FORMULATION

A. Expressions for energy, number, quadrupole moment and $B(E2)$

It is clear that the accurate calculation of the excited states of heavier nuclei from the microscopic many-body theory would require a large number of nucleons to be treated dynamically in a large configuration space. The computational difficulties involved in performing such projected HFB calculations can be somewhat reduced by employing a simpler many-body Hamiltonian. In this paper, we use the quadrupole plus pairing interaction Hamiltonian whose parameters are determined by Kumar and Baranger[8] from their study of equilibrium deformations of heavy nuclei:

$$H=\sum_{\alpha}\epsilon_{\alpha}a_{\alpha}^{\dagger}a_{\alpha}-\frac{\chi}{2}\sum\langle\alpha|q^{2\mu}|\gamma\rangle\langle\delta|q^{2\mu}|\beta\rangle a_{\alpha}^{\dagger}a_{\beta}^{\dagger}a_{\delta}a_{\gamma}$$
$$-\tfrac{1}{2}G\sum(-1)^{j_{\alpha}-m_{\alpha}+j_{\gamma}-m_{\gamma}}a_{\alpha}^{\dagger}a_{\bar{\alpha}}^{\dagger}a_{\bar{\gamma}}a_{\gamma}\,, \tag{1}$$

where $q^{2\mu}$ is the quadrupole operator and χ and G are the strengths of the quadrupole and pairing interactions, respectively. The subscript α in Eq. (1) denotes all the quantum numbers $(n_{\alpha}, l_{\alpha}, j_{\alpha}, m_{\alpha})$ necessary for the specification of a spherical single-particle state. The state $\bar{\alpha}$ is connected to the state α by a time reversal operator. The sums in Eq. (1) run over the entire configuration space.

We consider the intrinsic variational wave function to be axially symmetric in view of the fact that the nuclei under investigation are found[8,9] to prefer axially symmetric equilibrium deformation. It may also be mentioned here that the nonaxial variational state introduces further complexities which would make the projection calculations prohibitive in large configuration space. The trial variational wave function is taken to be the good angular momentum state projected from the intinsic BCS state $\Phi_0(\beta,\ \Delta_p,\ \Delta_n,\ \lambda_p,\ \lambda_n)$ of the A-nucleon system. The deformation β, the pairing gaps Δ_p (for protons) and Δ_n (for neutrons), and the chemical potentials λ_p (for protons) and λ_n (for neutrons) are the variational parameters for each angular momentum state J. The chemical potentials in any state J are determined such that the number in the projected state is equal to the actual number. The wave function $\Psi_M^J(\beta, \Delta_p, \Delta_n, \lambda_p, \lambda_n)$ projected from the intrinsic state Φ_0 is given by

$$\Psi_M^J=P_{M0}^J\Phi_0\,, \tag{2}$$

where P_{M0}^J is the angular momentum projection operator and

$$\Phi_0(\beta, \Delta_p, \Delta_n, \lambda_p, \lambda_n)=\prod_{i+}(u_i+v_i b_i^{\dagger}b_{i-}^{\dagger})\,|0\rangle\,. \tag{3}$$

The occupation probability $v_i^{\,2}=1-u_i^{\,2}$ is related to the pairing gap Δ and the chemical potential λ. The fermion operator $b_i^{\dagger}$ corresponding to the ith deformed single-particle state is obtained from the spherical state operators $a_{\alpha}^{\dagger}$ by the transformation

$$b_{i\pm}^{\dagger}=\sum(\alpha\pm|C|i\pm)a_{\alpha\pm}^{\dagger}\,. \tag{4}$$

It should be noted that the basis states are divided into two subsets that are connected by a time-reversal operator T:

$$T|\alpha+\rangle=(-1)^{l_{\alpha}+j_{\alpha}-m_{\alpha}}|\alpha-\rangle\,, \tag{5}$$

where $|\alpha\pm\rangle=|n_{\alpha}, l_{\alpha}, j_{\alpha}, \pm m_{\alpha}\rangle$. The transformation coefficients in Eq. (4) satisfy the relations

$$(\alpha-|C|i-)=(-1)^{l_{\alpha}+j_{\alpha}-m_{\alpha}}(\alpha+|C|i+)\,,$$
$$C\tilde{C}=\tilde{C}C=1\,, \tag{6}$$

where $\tilde{C}$ is the transpose of matrix C.

The expectation value E^J of the Hamiltonian in Eq. (1) with respect to the wave function in Eq. (2) is obtained by expressing the projection operator P_{M0}^J in terms of the rotation operator $R(\Omega)$ corresponding to the rotation through Euler angles $\Omega=(\Omega_1, \Omega_2, \Omega_3)$. Thus,

$$E^J(\beta, \Delta_p, \Delta_n, \lambda_p, \lambda_n) = h^J / p^J \,, \tag{7}$$

where

$$h^J(\beta, \Delta_p, \Delta_n, \lambda_p, \lambda_n) = \frac{2J+1}{8\pi^2} \int D^J_{00}(\Omega) \langle \Phi_0 | HR(\Omega) | \Phi_0 \rangle d\Omega \,, \tag{8}$$

and p^J is obtained from Eq. (8) by replacing H with 1. The matrix elements $\langle \Phi_0 | R | \Phi_0 \rangle$ and $\langle \Phi_0 | HR | \Phi_0 \rangle$, necessary for evaluating p^J and h^J, are given by

$$\langle \Phi_0 | R | \Phi_0 \rangle = (\det W)^{1/2} \,, \tag{9}$$

$$\frac{\langle \Phi_0 | HR | \Phi_0 \rangle}{\langle \Phi_0 | R | \Phi_0 \rangle} = 2 \sum_i{}' \epsilon_i \rho_{i+i+} - G\eta^2 - \frac{\chi}{2}(Q^{02}_+ + 2Q^{12}_- + 2Q^{22}_-) \,. \tag{10}$$

The matrix W in Eq. (9) is obtained in terms of the transformation matrix of Eq. (4), the rotation matrix D, and the diagonal matrices U and V corresponding to the vacancy and occupation probabilities in Eq. (2):

$$W = U\tilde{C}\tilde{D}^* C U + V\tilde{C}\tilde{D} C V \,. \tag{11}$$

The generalized density matrices appearing in Eq. (10) can now be expressed as

$$\rho = 1 - UW^{-1}U\tilde{C}\tilde{D}^* C \,, \qquad \sigma = \tilde{C}D^* C U \tilde{W}^{-1} V \tilde{C} \tilde{T} C \,. \tag{12}$$

The quantities Q and η in Eq. (10) are given by

$$Q^\mu_\pm = \sum{}' (q^{2\mu}_{i\pm j+} + q^{2\mu}_{j+i\pm}) \rho_{j+i\pm} \,, \qquad \eta = \sum{}' \sigma_{i+i-} \,. \tag{13}$$

The primes on the summations in Eqs. (10) and (12) indicate that the summation is only over one subset of states. The number of protons and the neutrons N^J in the projected state are obtained by evaluating the integral

$$Z^J(\beta, \Delta_p, \Delta_n, \lambda_p, \lambda_n) = \frac{2J+1}{4\pi^2 p^J} \int D^J_{00}(\Omega) (\det W)^{1/2} \sum_i{}' \rho_{i+i+} d\Omega \,. \tag{14}$$

The summation in Eq. (14) over proton (neutron) states gives the proton (neutron) number Z^J (N^J). The expression for the $B(E2; J_i \to J_f)$ value can also be easily derived and is given by

$$B(E2; J_i \to J_f) = \frac{2J_f+1}{2J_i+1} (p^{J_i} p^{J_f})^{-1} [Q(J_i \to J_f)]^2 \,, \tag{15}$$

where

$$Q(J_i \to J_f) = \sum_{\gamma=0}^{2} (2 - \delta_{\gamma 0}) (J_i 0, 20 | J_f 0) (2J_i + 1) \times \int_0^{\pi/2} d^{J_i}_{-\gamma 0}(\theta) (Q^\nu_+ + Q^\nu_-) (\det W)^{1/2} \sin\theta \, d\theta \,.$$

Here $(J_i O, 2O | J_f O)$ is the Clebsch-Gordan coefficient, and $Q^\gamma_\pm$ is given by Eq. (13).

B. Minimization procedure

The nuclear energies are calculated by minimizing E^J in Eq. (7) by varying the parameters β, Δ_p, Δ_n, λ_p, λ_n for each angular momentum state J. For each set of the values of β, Δ_p, and Δ_n, the chemical potentials λ_p and λ_n occurring in the definition of the U and V matrices are varied so as to yield the correct number Z^J of protons and N^J of neutrons for each J. The numbers Z^J and N^J computed from Eq. (14) are very sensitively dependent on λ_p and λ_n; consequently, it is necessary to incorporate very fine variations in λ_p and λ_n in the variational procedure so as to obtain the correct number in each angular momentum state. In the calculations reported in this paper, we have achieved an accuracy up to the fourth decimal place in the numbers computed in each state J.

C. Renormalization procedure

The parameters χ and G of the Hamiltonian of Eq. (1) employed in the present calculations are determined[8] from the consideration of the intrinsic states of the deformed nuclei in the region of interest. The values of the parameters are estimated[8] by considering the configuration space of two major shells and assuming an inert core with $Z=40$ and $N=70$. The assumption of inert core may need some modifications in connection with the yrast states projected from the intrinsic states of the nuclei. The simplest way to incorporate the effect of the neglected core on the projected energies is by renormalizing the calculated energy spectrum. We achieve it by introducing a parameter, namely the moment of inertia $\mathcal{I}_{\text{core}}$ of the core. Since one is attempting to explain a large amount of data, the introduction of an additional parameter is justified if it substantially improves the agreement with the data. Besides, the systematic behavior of the parameter may also provide interesting information on the intrinsic structure of the nucleus. We assume that the moment of inertia of the nucleus is the sum of the moment of inertia of the core and that of the outer nucleons. It is reasonable to assume that the core moment of inertia is independent of total angular momentum J at least for a set of

states, whereas the moment of inertia $\mathcal{I}_{\text{calc}}$ calculated by considering only the outer nucleons would depend on J as deduced from the computed energies E^J_{calc}. Thus,

$$E^J_{\text{calc}}=\frac{\hbar^2}{2\mathcal{I}_{\text{calc}}}J(J+1)\,. \tag{16}$$

The corrected or normalized energy is then given by

$$E^J_{\text{norm}}=\frac{\hbar^2 J(J+1)}{2(\mathcal{I}_{\text{core}}+\mathcal{I}_{\text{calc}})}\,. \tag{17}$$

One can, alternatively, express the renormalized energy as

$$E^J_{\text{norm}}=\frac{E^J_{\text{calc}}E^J_{\text{core}}}{E^J_{\text{calc}}+E^J_{\text{core}}}\,, \tag{18}$$

where E^J_{core} is obtained from an expression similar to that of Eq. (16) by replacing $\mathcal{I}^J_{\text{calc}}$ with $\mathcal{I}_{\text{core}}$. It is obvious from Eq. (18) that $E^J_{\text{norm}}\simeq E^J_{\text{calc}}$ if $E^J_{\text{core}}\gg E^J_{\text{calc}}$, and $E^J_{\text{norm}}\simeq E^J_{\text{core}}$ if $E^J_{\text{calc}}\gg E^J_{\text{core}}$.

III. RESULTS AND DISCUSSION

We have employed the nuclear Hamiltonian in Eq. (1) with the strength parameters χ and G determined by Kumar and Baranger.[8] The same configuration space and the same inert core as specified[8] by them has been considered in the present calculations. The theoretical formulation of Sec. II is used to calculate the energy spectra and the $B(E2)$ values of three erbium isotopes ^{158,160,162}Er. In order to study the influence of number projection on the deformation parameter β, pairing gaps Δ_p, Δ_n, and the computed energies, we have calculated the energy spectra in each of the three nuclei for the following three cases.

In the first case, the energy spectra are projected from the intrinsic Hartree-BCS state[8] corresponding to the equilibrium deformation β_0 with the relevant gap parameters Δ_{p0} and Δ_{n0} and the chemical potentials λ_{p0} and λ_{n0} determined from the number conservation in the intrinsic state. The wave function in this case will be denoted by $\Psi^J_1(\beta_0, \Delta_{p0}, \Delta_{n0}, \lambda_{p0}, \lambda_{n0})$. In the second case corresponding to the variational calculation without number conservation in the projected state, the energy spectra are obtained by minimizing the projected energy with respect to the variations in β, Δ_p, and Δ_n for each angular momentum state. The wave function in this case will be denoted by $\Psi^J_2(\beta, \Delta_p, \Delta_n, \lambda_{p0}, \lambda_{n0})$. The third case corresponds to a full variational calculation in which all the parameters β, Δ_p, Δ_n, λ_p, and λ_n are varied to obtain the minimum in energy and to achieve number conservation in each angular momentum state. The wave function in this case will be denoted by $\Psi^J_3(\beta, \Delta_p, \Delta_n, \lambda_p, \lambda_n)$. The energy spectra obtained in the three cases are exhibited in Table I.

It is observed from Table I that the projected energy spectra obtained in the first case reproduce the low-lying levels with $J\leq 6$ reasonably well in all the three nuclei but fail to reproduce the observed high spin states. This may be due to the choice of the interaction parameters which are fitted to reproduce the ground state and the first excited state of these nuclei. It should also be noted that in all the three nuclei (the variational calculation with wave function Ψ^J_2 of the second case yields a good agreement with the observed energies for $J\leq 6$ and for $J>6$) the agreement is better than that obtained in the first case with wave function Ψ^J_1. This could be attributed to the effect of large angular momentum on the de-

TABLE I. The calculated and experimental energy spectra are tabulated. The energies (in MeV) in the first four columns of each nucleus are obtained from the intrinsic BCS state, the variational state without number conservation, the variational state with number conservation, and the renormalization procedure, respectively.

	^{158}Er					^{160}Er					^{162}Er				
J	I	II	III	IV	Expt	I	II	III	IV	Expt	I	II	III	IV	Expt
0	0.00	0.00	0.00	0.00	0.00	0.00	0.00	0.00	0.00	0.00	0.00	0.00	0.00	0.00	0.00
2	0.17	0.17	0.30	0.16	0.19	0.15	0.15	0.18	0.12	0.13	0.14	0.14	0.18	0.11	0.11
4	0.54	0.54	0.90	0.50	0.53	0.48	0.48	0.60	0.38	0.38	0.47	0.47	0.57	0.34	0.35
6	1.09	1.09	1.70	0.98	0.97	0.98	0.98	1.23	0.79	0.78	0.97	0.97	1.13	0.69	0.69
8	1.74	1.67	2.50	1.53	1.50	1.62	1.58	1.92	1.28	1.26	1.63	1.59	1.81	1.13	1.14
10	2.46	2.24	3.28	2.13	2.08	2.39	2.28	2.63	1.81	1.81	2.41	2.31	2.56	1.65	1.63
12	3.25	2.60	3.48	2.74	2.68	3.27	2.95	3.33	2.37	2.39	3.31	3.11	3.33	2.21	2.15
14	4.09	2.92	3.94	3.22	3.19	4.23	3.59	3.96	2.92	2.95	4.29	3.74	3.94	2.72	2.70
16	4.89	3.30	4.41	3.69	3.67	5.26	4.22	4.59	3.48	3.49	5.36	4.39	4.58	3.27	3.23
18	5.65	3.78	4.98	4.24	4.23	6.35	4.92	5.30	4.10	4.03	6.49	5.12	5.30	3.90	
20	7.04	4.41	5.70	4.96	4.89	7.49	5.70	6.09	4.78		7.67	5.91	6.09	4.55	

formation and pairing gaps. The values of the deformation parameter β corresponding to the minimum of energy E^J are plotted as a function of J in Fig. 1. A similar plot of variation of pairing gaps Δ_p and Δ_n with angular momentum J is displayed in Fig. 2. The variational calculations show that β, Δ_p, and Δ_n corresponding to the minimum of energy for $J \leq 6$ are very close to β_0, Δ_{p0}, and Δ_{n0} obtained from the first type of calculation. For the states with $J=8$ and $J=10$, the deformation β and the pairing gap Δ_p for protons do not change. The pairing gap Δ_n for neutrons, however, starts decreasing, indicating that it is softer than Δ_p and β for changes with respect to the angular momentum J. As the angular momentum increases further with $J>10$, the neutron pairing gap Δ_n goes to zero rapidly with sudden changes in deformation. However, the proton gap Δ_p still changes very slightly up to $J=20$. This general feature is observed in all the three nuclei under investigation.

The near constancy of the proton pairing gaps Δ_p with angular momentum J is displayed in Fig. 2. It can be understood in view of the fact that the difference in the separation energy between the last occupied and the first excited single-particle proton states decreases only very slightly by $\simeq 0.5$ MeV as the deformation β changes from 0.24 to 0.32 in these erbium nuclei under consideration here. This is shown in Fig. 3. The important factor deciding the pairing gap is the separation energy between the last occupied and first excited single-particle state at the Fermi level. Since this separation does not change with deformation β and remains nearly the same for all values of J, the pairing gap Δ_p for protons does not vary with angular momentum in these erbium nuclei. In order to

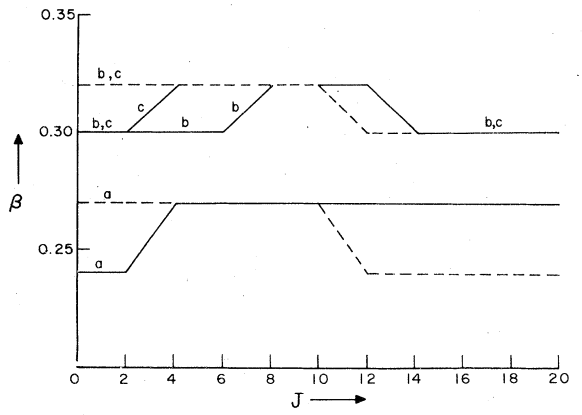

FIG. 1. The deformation β corresponding to the minimum in energy is plotted as a function of angular momentum J. The solid and dashed curved refer to the results with and without number conservation respectively. The curves a, b, and c refer to ^{158}Er, ^{160}Er, and ^{162}Er, respectively.

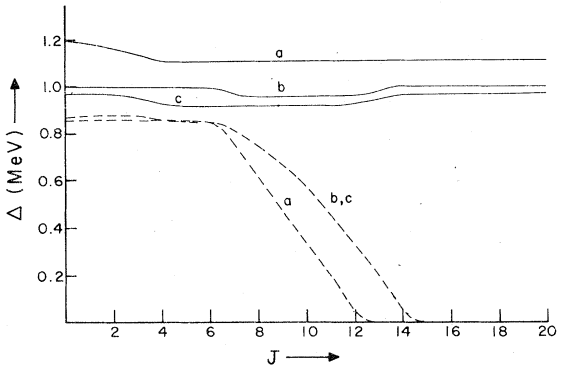

FIG. 2. The pairing gaps Δ_p for protons (solid curve) and Δ_n for neutrons (dashed curve) corresponding to the minimum in energy are plotted as functions of angular momentum J. The curves a, b, and c refer to ^{158}Er, ^{160}Er, and ^{162}Er, respectively.

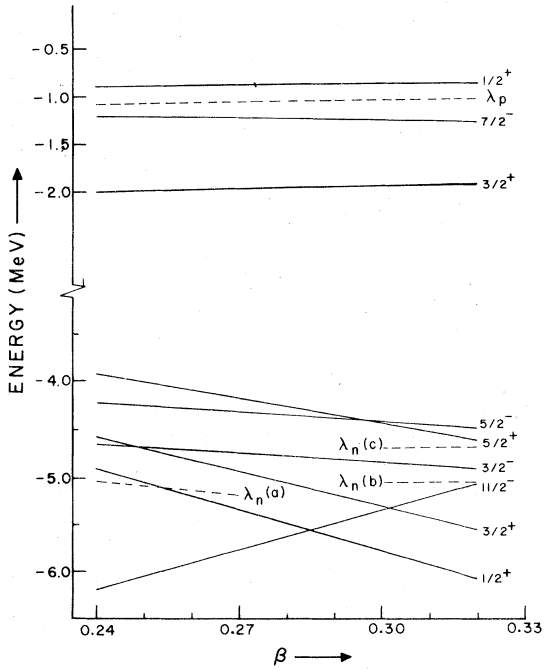

FIG. 3. The energies (in MeV) of the deformed orbitals near the Fermi levels λ_p for protons and λ_n for neutrons are shown as a function of deformation β. The λ_p and λ_n values for the three nuclei are indicated by a dashed curve. The Ω^π value of the orbit is shown on the right-hand side.

understand qualitatively the behavior of pairing gap Δ_n for neutrons, it should be noted from Fig. 1 that for $J>12$, the deformation β decreases at least in ^{160,162}Er. It should then be observed from Fig. 3 that the separation between the last occupied neutron state and the first excited neutron state increases with the decrease of deformation. It is thus expected that the pairing gap for neutrons decreases with an increase in J beyond $J>12$. Besides this implicit dependence on deformation, there would also be other angular momentum dependence arising from the variation after projection. This effect analogous to the Mottelson-Valatin effect[2] seems to be dominating in all the three nuclei ^{158,160,162}Er. The neutron pairing gaps approach zero very fast as seen from Fig. 2. The importance of this effect is explicitly demonstrated in the case of ^{158}Er, wherein Δ_n vanishes in spite of a small separation energy at the Fermi level for large angular momentum $J \gtrsim 14$.

It should be noted from Fig. 1 that the deformation β reduces for higher J in the case of variational calculations performed without number conservation. This behavior is contrary to the expectation that deformation would increase with the angular momentum. It is one of the intentions of the present investigations to find out whether this unexpected behavior is a result of the nonconservation of the number of nucleons. The effect of number conservation in each angular momentum state on the deformation β is shown in Fig. 1. It is clearly seen from Fig. 1 that the number conservation affects the deformation substantially. In fact, the trend of variation of deformation β with angular momentum J is just the opposite to that observed when the number conservation is not enforced. For a few low values of J, the deformation β obtained from the calculations with the wave functions Ψ_3^J with number conservation is smaller than that obtained from the calculations with wave functions Ψ_2^J without number conservation. The deformation β now increases for higher values of $J \gtrsim 4$, in contrast to the results of calculations without number conservation. This trend is observed in all the three nuclei considered in the present work. At still higher values of $J \gtrsim 14$, the deformation in ^{160,162}Er decreases back to the equilibrium deformation value, whereas it remains constant in ^{158}Er for all the higher J values. The present calculations thus clearly indicate that the number conservation significantly affects the deformation β. On the other hand, the number conservation does not affect the pairing gaps Δ_p and Δ_n. As seen from the results shown in Fig. 2, the pairing gaps, particularly the neutron gaps, have a very pronounced dependence on the angular momentum J. It is, however, found from the present calculations that the pairing gaps are almost insensitive to the small fluctuations in the number of nucleons. A similar behavior of deformation and pairing gaps with and without number conservation was observed[7] in the case of Yb isotopes.

The observed change in deformation due to number conservation is expected to affect the nuclear energy spectrum since the latter depends sensitively on the deformation. The energy spectra obtained from the present variational calculations with and without number conservation are shown in Table I. The energy spectra, as seen from Table I, change significantly after number conservation. The change, however, is in the wrong direction. The energy spectra obtained with number conservation are much more spread out than those obtained without number conservation, thus making the agreement with the experimental spectra poorer. It is seen from Table I that, in all the three nuclei, the energy spectra calculated without number conservation agree better with the experimental spectra as compared to those calculated with number conservation. This unexpected result could be attributed to the truncation of the configuration space and the assumption of an inert core. The effect of the "inert" core on the energy spectra can be incorporated by introducing the parameter $\mathcal{I}_{\text{core}}$ to account for the contribution of core

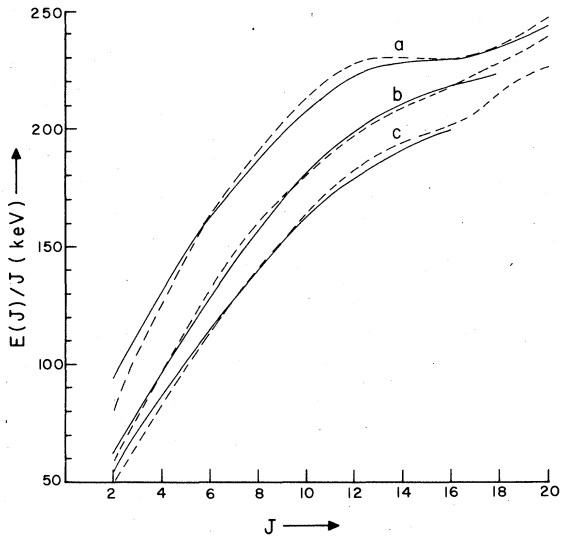

FIG. 4. The calculated (dashed cureve) and the experimental (solid curve) values of energy $E(J)/J$ (in keV) are plotted as a function of angular momentum J. The curves a, b, and c refer to ^{158}Er, ^{160}Er, and ^{162}Er, respectively.

polarization to the nuclear moment of inertia. The core polarization essentially renormalizes the energy spectrum as indicated in Sec. II C. The renormalized energies thus computed are shown in Table I. It is seen that these renormalized energy spectra are in excellent agreement with the corresponding experimental spectra in all the three nuclei under consideration. In order to visualize the agreement between the calculated and experimental energy spectra at a glance, we have plotted E^J/J as a function of J for the three erbium isotopes in Fig. 4. The good agreement is quite evident from this figure in which the energy is plotted on the keV scale. This figure also brings out the salient physical effect of a pronounced departure of the energy spectra from the simple rotational structure at around $J \simeq 12$. It should be remarked here that the renormalization in the case of energy spectra obtained without number conservation does not yield such an agreement with the experimental spectra as obtained with number conservation. The values of the moment of inertia $\mathcal{I}_{\text{core}}$ of the core employed in the renormalization calculations are, in the units of $\hbar^2$/MeV, 9.10 for ^{158}Er, 9.43 for ^{160}Er, and 11.63 for ^{162}Er. It is, however, observed that equally good agreement for all the states cannot be obtained by the same value $\mathcal{I}_{\text{core}}$ =9.10 in the case of ^{158}Er. The renormalized energies ^{158}Er shown in Table I are obtained with $\mathcal{I}_{\text{core}}$=9.10 for states with $J<12$ and with $\mathcal{I}_{\text{core}}$ =6.02 for states with $J \geq 12$. It should be noted that the moment of inertia increases with mass number from 9.10 in ^{158}Er to 11.63 in ^{162}Er. The sudden change in $\mathcal{I}_{\text{core}}$ value from 9.10 to 6.02 indicates that the nuclear core state in ^{158}Er changes at $J \simeq 12$.

The quadrupole moment $Q(J)$ and $B(E2;J+2 \rightarrow J)$ values are calculated by employing the three types of wave functions Ψ_1^J, Ψ_2^J, and Ψ_3^J described earlier. The core-polarization and truncation effects are simulated by ascribing the effective charges e_p=1.53e to the protons and e_n =0.53e to the neutrons. The computed $B(E2)$ values in the three nuclei under investigation are shown in Table II. The agreement between the calculated and the corresponding experimental $B(E2)$ values, as seen from Table II, is quite good. It should be noted from Table II that the $B(E2;J+2 \rightarrow J)$ values for $J \leq 8$ obtained from wave functions Ψ_1^J projected from the intrinsic BCS state $\Phi_0(\beta_0, \Delta_{p0}, \Delta_{n0}, \lambda_{p0}, \lambda_{n0})$ are identical with those obtained from the variational wave functions Ψ_2^J without number conservation. Calculations with the variational wave functions Ψ_3^J with number conservation show that the $B(E2)$ values for $J<4$ are decreased, whereas those for $4 \leq J \leq 8$ are almost unaffected. In the case of higher spins $J>10$, the situation is different. The $B(E2)$ values calculated from the wave functions Ψ_1^J are larger than the corresponding values obtained from variational wave functions Ψ_2^J. The number conservation does not change these values in ^{160,162}Er as seen from the almost identical

TABLE II. The calculated and experimental $B(E2;J+2 \rightarrow J)$ values in units of $e^2 \times 10^{-50}$ cm^4 are tabulated. Experimental values are from Ref. 10. The theoretical results in the first three columns of each nucleus are obtained with wave functions projected from the intrinsic BCS state, the variational wave functions without number conservation, and the variational wave functions with number conservation, respectively.

	^{158}Er				^{160}Er				^{162}Er		
J	I	II	III	Expt	I	II	III	Expt	I	II	III
0	68.4	68.4	58.7	$76.3^{+4.1}_{-3.6}$	92.4	92.4	83.7	$86.4^{+1.9}_{-1.8}$	94.9	94.4	87.6
2	98.3	98.3	84.6	$86.9^{+4.5}_{-4.2}$	130.5	130.5	119.9	$138.6^{+7.1}_{-6.5}$	135.1	135.1	125.5
4	109.3	109.3	109.5	$122.9^{+24.8}_{-17.6}$	144.1	144.1	132.6	$102.9^{+9.8}_{-8.3}$	149.3	149.3	149.3
6	116.0	115.7	115.9	$112.3^{+71.3}_{-31.4}$	151.6	152.3	152.3	$103.2^{+28.7}_{-18.4}$	158.9	156.7	156.9
8	120.7	117.5	118.5	$108.2^{+54.1}_{-54.1}$	156.5	156.9	156.9	$91.1^{+55.6}_{-25.1}$	161.8	161.4	161.4
10	125.0	105.0	121.7	>104.3	160.2	146.0	146.0		165.6	152.3	162.8
12	128.2	106.5	119.2	$78.4^{+24.4}_{-15.1}$	163.1	146.0	146.2		168.6	154.5	152.5
14	130.7	107.9	120.3	$131.1^{+71.5}_{-34.5}$	165.7	147.7	147.7		171.0	153.9	153.9
16	133.6	109.0	120.3	>68.7	167.7	148.7	148.7		173.2	154.9	154.9
18	135.0	110.0	121.3		169.5	149.5	149.5		175.0	155.8	155.8

values obtained with the wave functions Ψ_2^J and Ψ_3^J for the two nuclei. In ^{158}Er, however, the number conservation results in increasing the $B(E2)$ values for $J \geq 10$. These results on the $B(E2)$ values for the high spin states in ^{158,160,162}Er indicate that the number conservation would affect the calculated values only if it changes the deformation.

In order to understand the connection between the Bohr-Mottelson collective model and the microscopic approach followed here, we have calculated the intrinsic quadrupole moment Q_0 from the $B(E2;J+2 \rightarrow J)$ values as well as from the $Q(J)$ values using the following relations from the collective model:

$$B(E2;J+2 \rightarrow J) = \frac{15}{32\pi} \frac{(J+1)(J+2)}{(2J+3)(2J+5)} Q_0^2 ,$$
$$Q(J) = -\frac{J}{(2J+3)} Q_0 . \tag{19}$$

The calculated quadrupole moment $Q(J)$ along with the intrinsic quadrupole moments Q_0 extracted from Eq. (19) are displayed in Table III. It is clearly seen from Table III that in all the three erbium nuclei the values $Q_0(Q)$ extracted from the quadrupole moment $Q(J)$ agree very well with the corresponding value $Q_0(E2)$ obtained from the $B(E2;J+2 \rightarrow J)$ value. In general, $Q_0(Q)$ is slightly less than the corresponding $Q_0(E2)$ value as seen from Table III. One can also observe from Table III a systematic trend in the behavior of both Q_0 values as deformation changes for different angular momentum states. In ^{158}Er, the deformation is 0.24 for $J \leq 2$ and it changes to 0.27 for rest of the states up to $J=20$. The computed Q_0 values are found to be (Table III) nearly constant for all the states, except the $J=2$ state for which Q_0 value is lower than those for the rest of the states. This result is expected on the basis of deformation for these states. The variation of Q_0 with the deformation is also seen from the tabulated values in two other isotopes, ^{160,162}Er. In ^{160}Er, $Q_0(Q)$ is nearly constant for the states with $J \leq 6$ and $J \geq 14$ for which the deformation is the same ($\beta = 0.30$); the $Q_0(Q)$ value is slightly larger for the set of states with $8 \leq J \leq 12$ for which the deformation is also larger ($\beta = 0.32$). Thus, the observed variation of Q_0 with deformation and the near equality of $Q_0(Q)$ and $Q_0(E2)$ values computed from the present microscopic calculations indicates that the microscopic approach brings out the basic features of the Bohr-Mottelson collective model.

It is worthwhile to discuss the single-particle orbits occupied by the last pair of nucleons in the intrinsic wave function for each angular momentum state. This may give some insight into the phenomenological approach[3] based on decoupling of bands where the Coriolis effects in high-j single-particle orbits are assumed to play an important role. In our microscopic approach, however, it is difficult to separate the contributions arising from Coriolis effects, centrifugal stretching, or the particle-core coupling. Nevertheless, they are all included in the microscopic approach. One can look into the intrinsic wave function to find its characteristic features that could be compared with the phenomenological approaches. Since we have not incorporated the band mixing in the present microscopic calculations, we can only compare the structure of the ground band in the two approaches. For this

TABLE III. The calculated static quadrupole moment $Q(J)$ and the intrinsic quadrupole moments $Q_0(Q)$ and $Q_0(E2)$ extracted from the computed $Q(J)$ and $B(E2)$ values respectively, are tabulated. The tabulated quantities are in units of $e \times 10^{-24}$ cm^2.

	^{158}Er			^{160}Er			^{162}Er		
J	$-Q(J)$	$Q_0(Q)$	$Q_0(E2)$	$-Q(J)$	$Q_0(Q)$	$Q_0(E2)$	$-Q(J)$	$Q_0(Q)$	$Q_0(E2)$
2	1.55	5.41	5.45	1.85	6.47	6.50	1.89	6.61	6.64
4	2.13	5.85	5.92	2.35	6.46	6.51	2.50	6.86	6.91
6	2.34	5.84	5.95	2.58	6.46	6.81	2.74	6.86	6.92
8	2.46	5.83	5.93	2.85	6.77	6.83	2.89	6.86	6.93
10	2.53	5.83	5.96	2.95	6.77	6.53	2.98	6.85	6.89
12	2.58	5.81	5.86	3.01	6.77	6.49	3.03	6.83	6.63
14	2.62	5.79	5.86	2.91	6.44	6.50	2.97	6.57	6.63
16	2.65	5.80	5.84	2.94	6.43	6.49	3.00	6.56	6.63
18	2.68	5.80	5.85	2.96	6.42	6.49	3.02	6.54	6.63

purpose, we study the highest occupied single-particle orbits just below the Fermi levels corresponding to the chemical potentials λ_p and λ_n. As seen from Fig. 3, the last pair of protons occupies the $\Omega=\frac{7}{2}$ orbit in which the largest ($\simeq 99\%$) amplitude is of the $0h_{11/2}$ single-particle state. This is true for all the angular momentum states in the three nuclei under consideration. The situation in the case of neutrons is, however, different in the three nuclei. In the case of high spin states corresponding to $\beta=0.27$ in ^{158}Er, the last pair of neutrons occupies the $\Omega=\frac{1}{2}$ orbit just below λ_n and the largest amplitude in its wave function is that of $0i_{13/2}$ single-particle state. This situation persists till the end of the energy spectrum up to $J=20$. In ^{160}Er, the orbit occupied by the last neutron pair is $\Omega=\frac{11}{2}$ from the $0h_{11/2}$ single-particle state. This configuration remains unchanged for all the angular momentum states in ^{160}Er. In the case of ^{162}Er, the pair of neutrons just below λ_n is the $\Omega=\frac{3}{2}$ orbit in which both $0h_{9/2}$ and $1f_{7/2}$ single-particle states are almost equally mixed. However, the $\Omega=\frac{5}{2}$ orbit very close to the $\Omega=\frac{3}{2}$ orbit is also substantially occupied by the neutron pair and this $\Omega=\frac{5}{2}$ orbit has the largest (90%) amplitude from $0i_{13/2}$ single-particle state. Thus, the present microscopic calculations indicate the presence of single-particle orbitals with high j values near the Fermi level in the intrinsic structure of the high angular momentum states of these nuclei as pointed out by Stephen and Simon.[3] It should, however, be stressed that the highest occupied neutron state near the Fermi level is not necessarily the $0i_{13/2}$ state.

IV. CONCLUSION

The microscopic formalism of variation after projection is applied to study the high spin yrast states in three erbium isotopes ^{158,160,162}Er. The nuclear Hamiltonian employed in the calculations consists of quadrupole plus pairing interactions. The configuration space comprises two major shells for both protons and neutrons outside the "inert" core with $Z=40$ and $N=70$. The effect of core polarization is simulated by ascribing effective charges to the nucleons and by introducing moment of inertia of the core to renormalize the energy spectra. The deformation β, pairing gaps Δ_p and Δ_n and the chemical potentials λ_p and λ_n are varied to obtain the energy minimum and to conserve the number of protons and neutrons in each angular momentum state. The effect of number conservation on deformation, pairing gaps, energy spectra and $B(E2)$ values is studied. It is found that the number conservation significantly affects the deformation and the calculated energy spectra. The renormalized energy spectra obtained with number conservation in each angular momentum state are in very good agreement with the experimental energy spectra. The computed $B(E2)$ values are in good agreement with the available experimental data. The intrinsic quadrupole moment Q_0 extracted from the calculated quadrupole moments and the corresponding $B(E2)$ values is found to be nearly equal. The variation of Q_0 is correlated to the deformation parameter β. Thus, the present microscopic approach preserves the basic features of the Bohr-Mottelson collective model.

[1]J. Krumlinde, Nucl. Phys. A160, 471 (1971); D. R. Bes, S. Landowne, and M. A. J. Mariscotti, Phys. Rev. 166, 1045 (1968); M. A. J. Mariscotti, G. Scharff-Goldhaber, and B. Buck, *ibid.* 178, 1864 (1969).

[2]B. R. Mottelson and J. G. Valatin, Phys. Rev. Lett. 5, 511 (1960).

[3]F. S. Stephens and R. S. Simon, Nucl. Phys. A183, 257 (1972).

[4]K. Kumar, Phys. Scr. 6, 170 (1972); S. C. K. Nair and A. Ansari, Phys. Lett. 47B, 200 (1973); B. Banerjee, M. Mang, and P. Ring, Nucl. Phys. A215, 366 (1973).

[5]A. Faessler, F. Grummer, L. Lin, and J. Urbano, Phys. Lett. 48B, 87 (1974).

[6]M. R. Gunye and C. S. Warke, J. Phys. (to be published); C. S. Warke and M. R. Gunye, Phys. Rev. C 13, 859 (1976).

[7]F. Grummer, K. W. Schmid, and A. Faessler, Nucl. Phys. A239, 289 (1975).

[8]K. Kumar and M. Baranger, Nucl. Phys. A110, 529 (1968).

[9]M. R. Gunye, S. Das Gupta, and M. A. Preston, Phys. Lett. 13, 246 (1964); S. Das Gupta and M. A. Preston, Nucl. Phys. 49, 401 (1963).

[10]R. M. Diamond *et al.*, Phys. Rev. Lett. 22, 546 (1969).